# Prediction of chaos in a Josephson junction by the Melnikov-function technique

M. Bartuccelli and P. L. Christiansen
*Laboratory of Applied Mathematical Physics, The Technical University of Denmark, DK-2800 Lyngby, Denmark*

N. F. Pedersen
*Physics Laboratory I, The Technical University of Denmark, DK-2800 Lyngby, Denmark*

M. P. Soerensen
*IBM Forschungslaboratorium Zürich, Säumerstrasse 4, CH-8803 Rüschlikon, Switzerland*

(Received 9 April 1985)

The Melnikov function for prediction of Smale horseshoe chaos is applied to the rf-driven Josephson junction. Linear and quadratic damping resistors are considered. In the latter case the analytic solution including damping and dc bias is used to obtain an improved threshold curve for the onset of chaos. The prediction is compared to new computational solutions. The Melnikov technique provides a good, but slightly low, estimate of the chaos threshold.

## I. INTRODUCTION

For some years the topic of chaos in the rf-current-biased Josephson junctions has attracted much interest. The first papers in that field were probably the qualitative work by Belykh *et al.*[1] and the numerical work by Huberman *et al.*[2] Since then a number of authors have made numerical calculations,[3–6] electronic simulations,[7–12] and to a limited extent experiments on real junctions.[13–16] One of the things that characterizes almost all this work is the lack of analytical methods to predict the onset of chaos. This situation was recently changed by the analytical works of Genchev *et al.*[17] and Salam and Sastry,[18] who used the method of Melnikov integrals[18–21] to predict regions in the parameter plane where chaos occurs. Their work is in some sense an extension of the early work in Ref. 1 on the shunted-junction model, and in the same spirit equations are derived for various regions of the same qualitative behavior. Together with the work of Kautz and Monaco[3] it is the first step towards an analytical prediction of chaos in the rf-driven Josephson junction.

In this paper we review the results of Salam and Sastry from the point of view of Josephson-junction applications. For a detailed mathematical treatment we refer to the original mathematical literature.[18–21] Further, we extend the method of Melnikov functions to predict chaos in a Josephson junction with quadratic damping. This latter model—unlike the model with a linear resistor—has the advantage that analytical solutions are known in the absence of an applied rf signal, and the method of Melnikov functions requires fewer assumptions. For both models the analytical predictions are compared with numerical simulations.

The paper is organized in the following way: Section II A discusses the application of the Melnikov method to a Josephson junction with a linear damping resistor. Section II B discusses the case of a Josephson junction with a quadratic quasiparticle $I$-$V$ curve. This model is interesting for two reasons: (i) For high temperatures quadratic damping provides better agreement with experimentally measured $I$-$V$ curves than linear damping. (ii) A full analytical solution to the equation with quadratic damping is known. Consequently, the Melnikov technique for the case with an applied rf signal is more accurate than the corresponding case with linear damping. Finally, Sec. III contains our summary and conclusion.

## II. THE rf-DRIVEN JOSEPHSON JUNCTION

In the following we shall consider systems of ordinary differential equations of the form

$$\frac{d\mathbf{X}}{dt}=\mathbf{h}_0(\mathbf{X})+\epsilon\mathbf{h}_1(\mathbf{X},t,\epsilon)\ , \tag{1}$$

where $\mathbf{X}=(\phi,y)$, $\mathbf{h}_0=(f_0,g_0)$, and $\mathbf{h}_1=(f_1,g_1)$.

The analytical expression for the Melnikov function for systems of type (1) is[21]

$$M(t_0)=\int_{-\infty}^{+\infty}\mathbf{h}_0(\mathbf{X}_h(t-t_0))\wedge\mathbf{h}_1(\mathbf{X}_h(t-t_0),t)\times\exp\left[-\int_0^{t-t_0}\mathrm{tr}[D_x\mathbf{h}_0(\mathbf{X}_h(s))]ds\right]dt\ , \tag{2}$$

where $\mathbf{X}_h$ denotes the homoclinic orbit. Here the wedge product is defined by $\mathbf{X}\wedge\mathbf{Y}=X_1Y_2-X_2Y_1$ and $D_x$ denotes the partial derivative with respect to $X$. It is important to notice that in order to apply formula (2) it is necessary to know the so-called homoclinic orbits[21] for the unperturbed system ($\epsilon=0$).

The Melnikov function is proportional to $d(t_0)$, which is the separation between the unstable orbit $\mathbf{X}^u(t_0,t_0)$ and the stable one $\mathbf{X}^s(t_0,t_0)$ (see Fig. 1). If $M(t_0)$ has a simple zero and *is independent of* $\epsilon$ as in (2), then the local stable and unstable manifolds intersect transversally. The presence of such intersecting orbits implies that the Poincaré map has the so-called Smale-horseshoe chaos.[21] A Smale horseshoe contains a countable set of unstable periodic or-

 

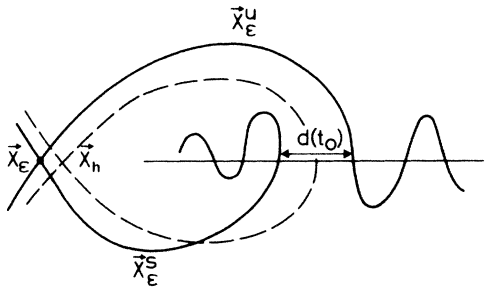


FIG. 1. Homoclinic orbit (dashed curve) and its perturbed curve (solid curve). Distance between trajectories, $d(t_0)$, is shown.

bits, an uncountable set of bounded nonperiodic orbits, and a dense orbit. It should be noticed that even though the Smale horseshoe is extremely complicated and contains an uncountable infinity of nonperiodic or chaotic orbits, it is not an attractor. However, it can exert a dramatic influence on the behavior of orbits which pass close to it. These orbits will display an extremely sensitive dependence upon initial conditions, and exhibit a chaotic transient before settling down to stable orbits of all periods which may constitute a strange attractor. Therefore the existence of the Smale horseshoe can be seen as the first step towards a possible chaotic behavior. Thus Melnikov's theory is expected to provide the lower boundary of the chaos threshold.

In the following we shall consider two different cases.

(i) Linear damping, which is the most commonly assumed case but for which an analytical solution to the unperturbed case (i.e., no applied rf signal) does not exist. Thus the conditions for the use of Melnikov's method are only approximately satisfied.

(ii) Quadratic damping, which in particular for high temperatures is a closer approximation to the $I$-$V$ curves in certain cases. This model has the important advantage that a full analytical solution in the absence of an applied rf signal is known.

### A. The Josephson junction with linear damping

The equation for a current-driven Josephson junction may be written[1-7]

$$\dot{\phi}=y \ , \qquad \dot{y}=-\sin\phi+\epsilon[\rho-\alpha y+\rho_1\sin(\Omega t)] \ . \tag{3}$$

Here the overdot indicates derivative with respect to time, $\alpha$ is the constant damping parameter, $\rho$ is the normalized dc bias current, $\rho_1$ is the normalized microwave current amplitude, and $\Omega$ is the applied frequency normalized to the Josephson plasma frequency. $\epsilon$ is a perturbative parameter that may eventually be set equal to 1, since in this case Melnikov's integral is $\epsilon$ independent.

The unperturbed system ($\epsilon=0$) is

$$\dot{\phi}=y \ , \qquad \dot{y}=-\sin\phi \ . \tag{4}$$

The heteroclinic orbits for the system [Eq. (4)] are given by

$$\phi_h(t-t_0)=\pm 2\tan^{-1}[\sinh(t-t_0)] \ , \qquad y_h(t-t_0)=\pm 2\,\mathrm{sech}(t-t_0) \ . \tag{5}$$

The Melnikov integral, Eq. (2), for the system (3) is

$$\begin{aligned} M(t_0)&=\int_{-\infty}^{+\infty} y_h(t-t_0)[\rho+\rho_1\sin(\Omega t)-\alpha y_h(t-t_0)]dt \\ &=\rho\int_{-\infty}^{+\infty} y_h(t)dt+\left[\rho_1\int_{-\infty}^{+\infty} y_h(t)\cos(\Omega t)dt\right] \\ &\quad\times\sin(\Omega t_0)-\alpha\int_{-\infty}^{+\infty} y_h^2(t)dt \ . \end{aligned} \tag{6}$$

Performing the integrals of Eq. (6) with the heteroclinic orbits, Eq. (5), the following result is obtained:

$$M(t_0)=\pm 2\pi\rho-8\alpha\pm 2\pi\rho_1\,\mathrm{sech}(\pi\Omega/2)\sin(\Omega t_0) \ . \tag{7}$$

Rearranging Eq. (7), we find a necessary condition for the intersection of the stable and unstable orbits to be[17,18]

$$|\pm\rho+4\alpha/\pi|\cosh(\pi\Omega/2)\leqq\rho_1 \ . \tag{8}$$

According to the previous discussion, Eq. (8) is a necessary condition for the existence of a Smale horseshoe. [The sufficient condition requires the existence of simple zeros of $M(t_0)$.] The formula deviates[22] from results in Ref. 18 by the factor $2/\Omega$. The condition is given in terms of the four parameters of the problem: $\rho$, $\alpha$, $\Omega$, and $\rho_1$. Numerically chaos has been investigated[2,4] in the $\Omega$-versus-$\rho_1$ plane for fixed $\alpha=0.2$ and $\rho=0$. Comparing in Fig. 2 the theory [Eq. (8)] and the simulations[2,4] for $\alpha=0.2$, we find that Eq. (8) predicts too low a threshold for chaos. Kautz and Monaco[3] speculate that intersections between stable and unstable manifolds exist everywhere above the line given by Eq. (8), but that the resulting chaotic orbit is unstable with respect to the zero-voltage state and thus not observed. The discrepancy may be illustrated by considering the case of small $\Omega$. For $\Omega<\alpha$ the impedance of the capacitor is very large and the circuit may be considered almost as if it were at dc. For $\rho=0$ the system is then well behaved at least up to $\rho_1=1$ (shown as the dashed line in Fig. 2). The trajectory in the

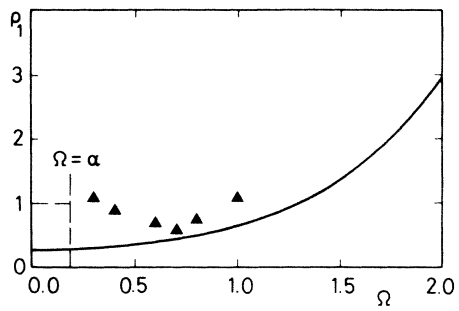


FIG. 2 Linear damping: threshold for chaos in parameter plane for $\rho=0$, $\alpha=0.2$. Solid curve: Eq. (8). Triangles: numerical results from Ref. 4.

phase plane is an ellipse centered at the equilibrium point (0,0). The voltage amplitude is approximately proportional to $\rho_1\Omega/(1+\alpha^2\Omega^2)^{1/2}$, which tends to zero as $\Omega\to 0$. For $\Omega=\alpha$, the impedance of the capacitor is the same as that of the resistor, and the capacitor can no longer be neglected.

For $\rho\neq 0$ very few systematic investigations exist, because the parameter space is four dimensional; however, Refs. 3, 5, and 6 contain numerical results, which can be compared with results obtained here. The structure of Eq. (8) is interesting and may be qualitatively understood from the following simple arguments. The lowest threshold of the applied rf current depends on the separation of the dc bias current from the quantity $\rho_c=4\alpha/\pi$. From other investigations[1] it is known that $\rho_c$ is the lowest bias current where rotating pendulum solutions exist; for this particular value of the bias current the trajectories for rotating and oscillating solutions of the pendulum equation get close to each other in the phase plane. Thus, for bias currents close to $\rho_c$ a very small perturbation may shift the system from one orbit to the other, i.e., the threshold for the applied rf current is lowest.

We may summarize the findings for the case of the linear resistor by saying that numerically $\rho$ should be within a band of magnitude $\Delta\rho$ given by

$$\Delta\rho=\rho_1\,\mathrm{sech}(\pi\Omega/2) \tag{9}$$

centered at $\rho_c$ in order to obtain horseshoe chaos. Figure 3 shows this band in the $\alpha$-versus-$\rho$ plane. $\rho_c=4\alpha/\pi$ separates regions of qualitatively different behavior in the parameter plane of the unperturbed system. For $\rho<\rho_c$ only oscillating solutions exist. For $\rho_c<\rho<1$ oscillating and rotating solutions exist, and for $\rho>1$ only rotating solutions exist. For large $\alpha$, $\rho_c$ is known to deviate from $\rho_c=4\alpha/\pi$ as shown in the figure. How the chaotic band develops for large $\alpha$ is outside the scope of the present paper. Here we only notice that the chaotic band follows the linear portion of the $\rho_c$ curve for low $\alpha$.

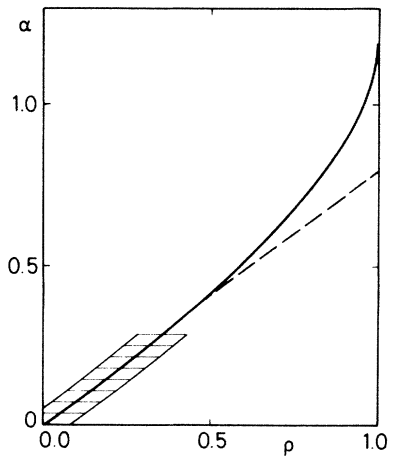


FIG. 3. Bifurcation diagram. Dashed curve: $\rho_c=4\alpha/\pi$. Solid curve: $\rho_c$ from numerical simulation. Crosshatched area: region of chaos.

### B. The Josephson junction with quadratic damping

If in the system (3) it is assumed that the resistance varies with the voltage such that $R=\mathrm{const}/V=(\hbar\gamma/2e)/V$, one obtains,[23] with the same normalization as in the system (3),

$$\ddot{\phi}+k(\dot{\phi})^2+\sin\phi=\rho+\rho_1\sin(\Omega t)\ , \tag{10}$$

where $k=(\gamma C)^{-1}$. Unlike the case with linear damping the exact analytical solution to Eq. (10) with $\rho_1=0$ has been obtained.[23] Introducing $y=\dot{\phi}$ one gets

$$\frac{dy^2}{d\phi}+2ky^2=2\rho-2\sin\phi \tag{11}$$

with the complete solution (assuming $\rho>0$)

$$y^2=\rho/k+4/(1+4k^2)^{1/2}\cos(\phi+\beta)+C_1\exp(-2k\phi)\ , \tag{12}$$

where $\tan\beta=2k$ and $C_1$ is an integration constant to be adjusted by the initial condition. Looking for the steady-state solution at finite voltages the transient term vanishes and Eq. (12) becomes

$$y^2=y_0^2[\rho+\rho_0\cos(\phi+\beta)]\ , \tag{13}$$

where $\rho_0=2k/(1+4k^2)^{1/2}$ and $y_0=k^{-1/2}$. If the voltage $\dot{\phi}$ goes negative, the damping term in Eq. (10), $k\dot{\phi}^2$, should be replaced by $k\,|\dot{\phi}|\,\dot{\phi}$. However, the solution to the resulting equation for $\dot{\phi}<0$ is obtained by a simple symmetry argument. We may note there that the parameter $\rho_0$ has the same physical meaning as the parameter $\rho_c$ defined for the linear resistor. Inserting $y=\dot{\phi}$ and rearranging, we may express the solutions to Eq. (13) in terms of elliptic functions.[24] For $\rho>\rho_0$ we get

$$(\phi+\beta)/2=\mathrm{am}(u),\quad \frac{d\phi}{dt}=\dot{y}=y_0(\rho+\rho_0)^{1/2}\mathrm{dn}(u)\ . \tag{14}$$

Here am is the amplitude function and dn is the Jacobian elliptic function of argument $u=(y_0/2)(\rho+\rho_0)^{1/2}(t-t_0)$ and modulus $m=2/(1+\rho/\rho_0)$. The trajectory of the solution, Eq. (14), is shown in Fig. 4 for $\rho=\rho_0$, and for $\rho$ slightly larger than $\rho_0$. To proceed we write Eq. (10) as the two-dimensional vector field,

$$\begin{aligned}\dot{\phi}&=y\ ,\\ \dot{y}&=-\sin\phi-k\dot{\phi}^2+\rho+\epsilon r_1\sin(\Omega t)\ .\end{aligned} \tag{15}$$

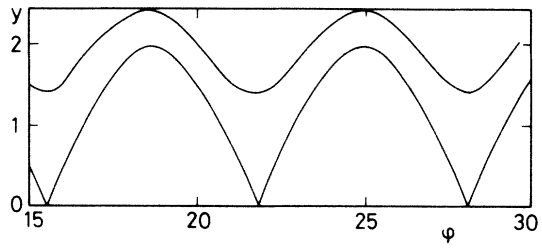


FIG. 4. Phase plane trajectories of Eq. (14) with $k=0.1$. Upper curve: $\rho=0.2$. Lower curve: heteroclinic orbit for $\rho=\rho_0=0.196$.

In the following we shall use the analytic solution, Eq. (14), to obtain the transverse intersections of the stable and unstable manifolds by finding the zeros of the Melnikov function. In order to do that it was noted in Sec. II that it is necessary to have a heteroclinic orbit for the unperturbed system ($\epsilon=0$) connecting hyperbolic saddle points. So we must investigate the fixed points of Eq. (13) when $\rho=\rho_0$. The fixed points are situated on the $\phi$ axis of the phase plane $(\phi,y)$. It is known[19–21] that the vector field $(\dot{\phi},\dot{y})$ should vanish at these points. This is found to be the case (i.e., $\dot{\phi}$ and $\dot{y}$ are simultaneously zero) in Eq. (14) for $\rho=\rho_0$. Further, we shall show that the equilibrium points of the vector field $(y,\dot{y})$ [Eq. (15) with $\epsilon=0$] are of the center type at

$$(\tilde{\phi},\tilde{y})=(-\sin^{-1}(\rho)+2n\pi,\ 0),\quad n=0,\pm1,\pm2,\ldots, \tag{16}$$

and of the saddle type at

$$(\tilde{\phi},\tilde{y})=(-\sin^{-1}(\rho)+(2n+1)\pi,\ 0),\quad n=0,\pm1,\pm2,\ldots. \tag{17}$$

We restrict the discussion to the equilibrium points in the interval

$$-\pi-\beta\leqq\phi\leqq\pi-\beta\ . \tag{18}$$

This means that we consider values of $\rho$ such that $\rho\leqq1$. For $\rho=\rho_0$ we find from Eq. (14) that $m=1$, and the limiting values of the elliptic functions are given by[24]

$$\mathrm{dn}(u,1)=\mathrm{sech}(u)\ \text{ and }\ \mathrm{am}(u,1)=\mathrm{gd}(u)\ , \tag{19}$$

where $\mathrm{gd}(u)$ denotes the Gudermannian function. In order to get more information on the behavior of the system about the point $\rho=\rho_0$, and in order to use the simple functions in Eq. (19), we rewrite Eq. (15) by adding a perturbation term $\Delta\rho=\rho-\rho_0=\epsilon(r-r_0)$ to obtain

$$\begin{aligned}\dot{\phi}&=y\ ,\\ \dot{y}&=-\sin\phi-k(\dot{\phi})^2+\rho_0+\epsilon[r_1\sin(\Omega t)+(r-r_0)]\ .\end{aligned} \tag{20}$$

For $\epsilon=1$, Eqs. (15) and (20) are identical. For $\epsilon=0$ we obtain the following heteroclinic orbit by using Eq. (19):

$$[\phi_h(t),y_h(t)]=\{4\tan^{-1}[\exp(bt/2)]-\beta-\pi,\ b\,\mathrm{sech}(bt/2)\}\ , \tag{21}$$

where $b=y_0(2\rho_0)^{1/2}$. The Melnikov integral is then given by [Eq. (2)]

$$M(t_0)=\int_{-\infty}^{\infty} b\,\mathrm{sech}[b(t-t_0)/2][\rho-\rho_0+\rho_1\sin(\Omega t)]\times\exp\left[\int_0^{t-t_0}2kb\,\mathrm{sech}(at'/2)dt'\right]dt\ . \tag{22}$$

Evaluating Eq. (22), we find

$$M(t_0)=(\rho-\rho_0)\sinh(2\pi k)/k+\rho_1 b\,[F_1\cos(\Omega t_0)+F_2\sin(\Omega t_0)]\ , \tag{23}$$

where

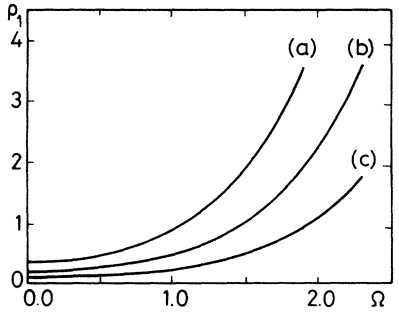


FIG. 5. Quadratic damping: Threshold for chaos in parameter plane [Eq. (24)]. (a) $\rho=0$, $k=0.2$; (b) $\rho=0$, $k=0.1$; and (c) $\rho=0.1$, $k=0.1$. Chaos above curves.

$$F_1=\int_{-\infty}^{\infty}\mathrm{sech}(bt/2)\sin(\Omega t)\times\exp\{4k\tan^{-1}[\sinh(bt/2)]\}dt$$

and

$$F_2=\int_{-\infty}^{\infty}\mathrm{sech}(bt/2)\cos(\Omega t)\times\exp\{4k\tan^{-1}[\sinh(bt/2)]\}dt\ .$$

It is easy to see that the integrals, $F_1$ and $F_2$, are finite and not zero. It is also possible to see that transversal zeros for the Melnikov function, Eq. (23), exist. A necessary condition is

$$\rho_1>(\rho-\rho_0)\sinh(2\pi k)/kb(F_1^2+F_2^2)^{1/2}\ . \tag{24}$$

The prediction for the onset of horseshoe chaos, Eq. (24), is plotted in Fig. 5 as a function of $\Omega$ for different values of parameters $\rho$ and $k$. Note that the structure of Eq. (24) is similar to that of Eq. (8). In Eq. (24), $\rho_0$ has the same significance as $\rho_c=4\alpha/\pi$ in Eq. (8), and the threshold rf current depends on the separation between $\rho$ and $\rho_0$.

Alternatively, one might derive a condition for intersecting perturbed heteroclinic orbits by considering also the loss and bias terms as perturbations and use the heteroclinic orbit in Eq. (5) for insertion into the Melnikov function. The calculation proceeds in the same manner as for the linear resistor and the result is a thresh-

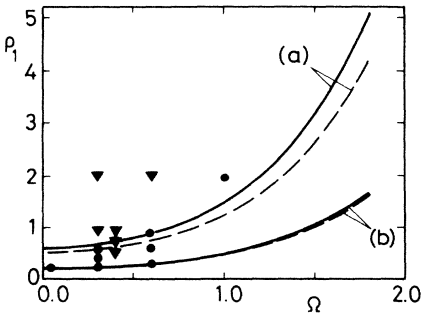


FIG. 6. Quadratic damping: Threshold for chaos in parameter plane for $\rho=0$. Solid curves: Eq. (25); dashed curves: Eq. (24). (a) $k=0.3$; (b) $k=0.1$. Numerical results for $k=0.1$: Triangles, chaotic solutions; circles, periodic solutions.

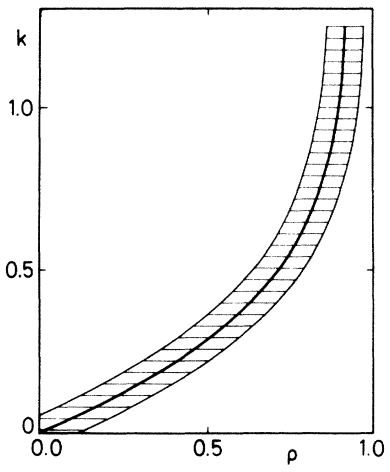


FIG. 7. Bifurcation diagram. Solid curve: $\rho_0=2k(1+4k^2)^{1/2}$ as defined in Eq. (13). Crosshatched area: region of chaos.

old condition given by

$$\rho_1 \geqq | \pm\rho+2k | \cosh(\pi\Omega/2) , \tag{25}$$

which is identical with Eq. (8), except that $2k$ replaces $4\alpha/\pi$. For small values of the loss one should expect Eqs. (24) and (25) to give identical results. In fact, the expansion of Eq. (24) to first order in the damping constant $k$ is identical with Eq. (25). Equation (24) may be considered a more precise condition since it is derived from the heteroclinic orbit to the unperturbed solution when both loss and bias are taken into account. Figure 6 shows a comparison between Eqs. (24) and (25) for $k=0.3$. A comparison between Eqs. (24) and (25) for $k=0.1$ and some corresponding numerical simulations are also shown. We note that the Melnikov function gives too low a boundary for the onset of chaos as in Fig. 2. An equation similar to Eq. (24) cannot be derived for the case of linear damping, since the solution to the unperturbed system is not known at present.

For the case of a quadratic damping term it is possible to make a similar discussion as that in connection with Fig. 3. Here, however, the analytic expression for the $\rho_0$ curve is known [Eq. (13)]. For $k\to\infty$ it approaches unity asymptotically. The band corresponding to chaos is given by

$$\Delta\rho=\rho_1 bk(F_1^2+F_2^2)^{1/2}/\sinh(2\pi k) , \tag{26}$$

which is shown crosshatched in Fig. 7.

## III. SUMMARY AND CONCLUSION

Chaos in the rf-driven Josephson junction was investigated analytically by means of the Melnikov-function technique. With a linear damping resistor only an approximate solution for the unperturbed phase plane trajectory could be used in the Melnikov integral. For the case of a quadratic damping term the analytic solution to the unperturbed case has been used, and an improved threshold curve for the onset of chaos has been obtained. For both cases, however, the Melnikov prediction gives a threshold somewhat lower than that found by direct computation. That is because the Smale horseshoe, whose existence in the Poincaré map is predicted by Melnikov's theory, is not an attractor; indeed the set of points asymptotic to it will have zero measure. Thus the existence of Smale horseshoe does not imply that typical trajectories will be asymptotically chaotic. In fact, in some cases we have transient chaos followed by asymptotically periodic motions. However, it may happen that some of the orbits constitute a strange attractor. Therefore the "presence" of the Smale horseshoe is the starting point over which a system can undertake some of the possible routes to chaos. Apparently the method seems to fail for low applied frequencies. Although the Melnikov technique seems to give a good estimate of the chaos threshold, further work is needed to obtain a detailed analytical criterion.

## ACKNOWLEDGMENTS

The financial support of the European Research Office of the United States Army (through Contract No. DAJA-37-82-C-0057) and the Consiglio Nazionale delle Ricerche (Italy) for one of the authors (M.B.) is gratefully acknowledged.

[1]V. N. Belykh, N. F. Pedersen, and O. H. Soerensen, Phys. Rev. B **16**, 4853 (1977); **16**, 4860 (1977).
[2]B. A. Huberman, J. P. Crutchfield, and N. H. Packard, Appl. Phys. Lett. **37**, 750 (1980).
[3]R. L. Kautz and R. Monaco, J. Appl. Phys. **57**, 875 (1985).
[4]N. F. Pedersen and A. Davidson, Appl. Phys. Lett. **39**, 830 (1981).
[5]R. L. Kautz, IEEE Trans. Magn. **MAG-19**, 465 (1983).
[6]Kazuo Sakai and Y. Yamaguchi, Phys. Rev. B **30**, 1219 (1984).
[7]I. Goldhirsch, Y. Imry, G. Wasserman, and E. Ben-Jacob, Phys. Rev. B **29**, 1218 (1984).
[8]D. D'Humières, M. R. Beasley, B. A. Huberman, and A. Libchaber, Phys. Rev. B **26**, 3483 (1982).
[9]M. Cirillo and N. F. Pedersen, Phys. Lett. **90A**, 150 (1982).
[10]H. Seifert, Phys. Lett. **98A**, 213 (1983).
[11]Da-Ren He, W. J. Yeh, and Y. K. Kao, Phys. Rev. B **30**, 172 (1984).
[12]V. K. Kornev and V. K. Semenov, IEEE Trans. Magn. **MAG-19**, 633 (1983).
[13]V. N. Gubankov, K. I. Konstantinyan, V. P. Koshelets, and G. A. Ovsyannikov, IEEE Trans. Magn. **MAG-19**, 637 (1983).
[14]R. F. Miracky and J. Clarke, Appl. Phys. Lett. **43**, 508 (1983).
[15]D. C. Cronemeyer, C. C. Chi, A. Davidson, and N. F. Pedersen, Phys. Rev. B **31**, 2667 (1985).
[16]M. Octavio, Phys. Rev. B **29**, 1231 (1984); M. Octavio and C. Readi Nasser, *ibid.* **30**, 1586 (1984).
[17]Z. G. Genchev, Z. G. Ivanov, and B. N. Todorov, IEEE Trans. Circuits Syst. **CAS-30**, 633 (1983).
[18]F. M. A. Salam and S. S. Sastry, *Chaos in Nonlinear Dynami-*

*cal Systems,* edited by J. Chandra (Society For Industrial and Applied Mathematics, Philadelphia, 1984), p. 43.
[19]V. K. Melnikov, Trans. Moscow Math. Soc. **12**, 1 (1963).
[20]V. I. Arnold, Sov. Math. Dokl. **5**, 581 (1964).
[21]J. Guckenheimer and P. J. Holmes, *Nonlinear Oscillation, Dynamical System, and Bifurcation of Vector Fields,* Vol. 42 of *Applied Mathematical Sciences* (Springer-Verlag, Berlin, 1983).
[22]The authors have informed us that this error will be corrected in a later version [IEEE Trans. Circuits Syst. (to be published)].
[23]N. F. Pedersen and K. Saermark, Physica **69**, 572 (1973).
[24]P. F. Byrd and M. D. Friedman, *Handbook of Elliptic Integrals for Engineers and Scientists* (Springer-Verlag, New York, 1971).